1 **Application of a multiphase microreactor chemostat for the determination of**

2 **reaction kinetics of *Staphylococcus carnosus***

3

4 S. Lladó Maldonado[1,2], J. Krull[1,2], D. Rasch[1,2], P. Panjan[3], A.M. Sesay[3], M.P.C. Marques[4], N. Szita[4],

5 R. Krull[1,2]

6 [1]Institute of Biochemical Engineering, Technische Universität Braunschweig, Braunschweig, Germany

7 [2]Center of Pharmaceutical Engineering (PVZ), Technische Universität Braunschweig, Braunschweig,

8 Germany

9 [3]Measurement Technology Unit, CEMIS-Oulu, Kajaani University Consortium, University of Oulu,

10 Kajaani, Finland

11 [4]Department of Biochemical Engineering, University College London, United Kingdom

12

13

14

15 Corresponding author:

16 Rainer Krull

17 Institute of Biochemical Engineering, Technische Universität Braunschweig

18 Rebenring 56, 38106 Braunschweig, Germany

19 Tel.: +49 (0)531/391-55311

20 Fax: +49 (0)531/391-55313

21 E-mail: r.krull@tu-braunschweig.de

22 **Abstract**

23 Bioreactors at the microliter-scale offer a promising approach to accelerate bioprocess development.
24 Advantages of such microbioreactors include a reduction in the use of expensive reagents. In this
25 study, a chemostat operation mode of a cuvette-based microbubble column-bioreactor made of
26 polystyrene (working volume of 550 µL) was demonstrated. Aeration occurs through a nozzle (Ø ≤
27 100 µm) and supports submerged whole-cell cultivation of *Staphylococcus carnosus*. Stationary
28 concentrations of biomass and glucose were determined in the dilution rate regime ranging from 0.12
29 to 0.80 1/h with a glucose feed concentration of 1 g/L. For the first time reaction kinetics of
30 *S. carnosus* were estimated from data obtained from continuous cultivation. The maximal specific
31 growth rate (μ_{max} = 0.824 1/h), Monod constant (K_S = $34 \cdot 10^{-3}$ g_S/L), substrate-related biomass yield
32 coefficient ($Y_{X/S}$ = 0.315 g_{CDW}/g_S), and maintenance coefficient (m_S = 0.0035 g_S/($g_{CDW} \cdot$h)) were
33 determined. These parameters are now available for further studies in the field of synthetic biology.

34

35 Keywords: Chemostat, reaction kinetics, microbioreactor, microbubble column-bioreactor,
36 *Staphylococcus carnosus*

1 Introduction

Bioprocesses involve the use of microorganisms or their constituent parts, such as enzymes, as a catalyst for producing valuable substances such as recombinant proteins, drugs or bio-based chemicals. Conventional methods for bioprocess development use extensive experiments at the laboratory scale to select the best cell metabolism conditions to improve productivity. These screening processes are not easy to parallelise and require time for experimentation and chemical analysis and a large number of samples, which leads to the generation of waste. Consequently, there is a great need for high-throughput devices that allow rapid and reliable bioprocess development, for instance, microbioreactors (*MBRs*). *MBRs* are miniaturised bioreactors with a working volume below 1000 µL [1]. The main advantages of *MBR*s are the minimization of space, reagents, their easy parallelization together with the integration of analytical tools makes them very interesting devices to develop bioprocesses with high–throughput screening potential [2, 3]. Therefore, the employment of *MBRs* represents a significant step to accelerate bioprocess research, optimising the cultivation conditions, and consequently increasing productivity at large scale. Since it is not trivial to insert standard electrodes (for example because of their size), and since continual sampling for at- or offline-HPLC measurements would rapidly deplete the cultivation medium of a *MBR*, integration of miniaturised sensors are typically preferred for monitoring the process conditions [4–8]. They offer online and real time monitoring of several cultivation variables, reduce or eliminate the need for sampling, avoid sample loss and contamination, and thus significantly reduce laboratory effort.

Most current *MBRs* operate in batch and fed-batch modes [9–15]. At these operation modes, the properties of microorganisms, such as size, compositions, and functional characteristics, vary significantly during growth and cultivation [16]. Steady state cell growth, in which cell biomass, substrates and product concentrations remain constant over cultivation time, can only be realized in continuous cultivation experiments. In a chemostat, the growth-limiting (chemical) substrate is continuously added and removed and is ensured through a constant concentration in the feed flow. Equal influent and effluent flow rates are maintained to retain a constant working volume. As a result, the cells are kept at a steady state with a constant growth rate and metabolic activity. This makes a chemostat an ideal experimental setup to study microbial systems. One of the most important features of the chemostat is that it allows the operator to control the cell growth rate by adjusting the dilution rate (*D*), which is the ratio of the flow rate divided by the cultivation volume. The major disadvantages of chemostat cultivations are the high amount of substrate needed to maintain long cultivation periods. This can be prohibitive when expensive substances are used. Some strategies to accelerate the experimental procedures and to reduce the substrate consumption are the use of parallel bioreactors [17], and the procedure followed here using *MBR*s [18–20].

Due to the low oxygen solubility in aqueous cultivation media and the high demand from aerobic bioprocesses, the supply of oxygen to microorganisms is the most critical transport process and may lead to mass transfer limitations. To overcome this challenge, previous *MBR* research using a microbubble column (*µBC*) for biotechnological screening purposes was performed by Peterat et al. [10] and Krull and Peterat [18] with the development and validation of a polydimethylsiloxane (*PDMS*)

76 -glass based *μBC* manufactured by soft lithography technology. Lladó Maldonado et al. [21] developed

77 a borosilicate glass based *μBC* manufactured by powder blasting and wet etching technology. The

78 active aeration of the *μBCs* allowed the proper oxygenation of the cultivation broth and ensured the

79 homogenization of the cultivation broth and prevented cell sedimentation. Recently, Lladó Maldonado

80 et al. [22] showed the development of a fully online sensor-equipped, disposable, multiphase *μBC*

81 (with a working volume of 550 μL) as a screening platform for biotechnological research purposes. Its

82 validation by batch cultivation of *Saccharomyces cerevisiae* proved the long-term functionality of the

83 reactor and the sensors (optical density, dissolved oxygen, pH and glucose) and established that the

84 evolution of process variables could be observed over time [22]. The *μBC* showed suitable aeration

85 characteristics with volumetric liquid-ph ase mass transfer coefficients, k_La, between 204 and 775 1/h.

86 The values for the k_La varied depending on the applied airflow rate, the composition of the cultivation

87 media, and the mixing time which ranged between 1 and 3 s.

88 Based on these advances, in the current study the operation of the above-mentioned rapid custom-

89 made and sensor-equipped *μBC* is shown with its application as a platform for cultivation of

90 *Staphylococcus carnosus* both in batch and chemostat mode. We show for first time, reaction kinetic

91 parameters of *S. carnosus* estimated from stationary concentrations of biomass and glucose obtained

92 from continuous cultivation experiments.

93 *S. carnosus* as a model organism is a non-pathogenic Gram-positive, facultatively anaerobic

94 staphylococcal species, which evolved over several decades to become an important strain in the food

95 engineering industry and is used as a starter culture in sausage production and has become a

96 versatile and powerful microbial tool in modern microbiology and biotechnology. The straightforward

97 translocation of recombinant proteins over the single cell membrane in Gram-positive bacteria

98 combined with the very low proteolytic extracellular activity makes *S. carnosus* an attractive host for

99 the production of secreted recombinant proteins [23]. Due to its properties, previous studies with the

100 same strain of *S. carnosus* were already performed at the microlitre-scale by Davies et al. [24] in a

101 *MBR* "cassette."

102

103 **2 Materials and Methods**

104 *2.1 Microbioreactor and experimental setup*

105 The *μBC* used in the experiments was developed and validated by Lladó Maldonado et al. [22]. It is

106 based on a semi-micro cuvette made of polystyrene (BR759015, Brand, Wertheim, Germany) that was

107 vertically cut in half through the *xy* plane. A polymethyl methacrylate (*PMMA*) microscope slide

108 (MS50510415, Labor-und Medizintechnik, Dr. Jutta Rost, Leipzig, Germany) was used to close the

109 vertical open side of the *μBC*. A modified needle (Sterican, B. Braun Melsungen AG, Melsungen,

110 Germany) with an outer diameter of 600 μm and an inner diameter manually reduced to less than

111 100 μm was inserted and sealed at the bottom of the cuvette, which served as a nozzle for the

112 compressed air supply. The *μBC* consisted of a reaction chamber (4 mm width, 5 mm depth, and

113 20 mm height) and a funnel at the upper part (10 mm width, 5 mm depth, and 25 mm height) to ensure

114 an adequate gas/liquid phase separation and provided a total volume of 1.5 mL. The *μBC* was filled

115   with cultivation medium up to the outlet level, which resulted in a final working volume of
116   approximately 550 µL (**Fig. 1**).

117   The experiments were performed in a custom-made incubation chamber (450 mm x 750 mm x
118   450 mm) that had temperature control as described in Peterat et al. [10] and Krull and Peterat [18]. To
119   avoid evaporation, the air supplied through the nozzle was water-saturated. The air flow was
120   conducted through a bottle (500 mL) filled with 50 % distilled water at a temperature of 30 °C to
121   ensure that the air flow did not have a cooling effect on the cultivation broth.

122   For the continuous cultivation the feed flow was injected through the inlet of the µBC by using a
123   precision syringe pump (neMESYS; Cetoni GmbH, Korbussen, Germany) in dispensing mode. The
124   flow in the outlet was suctioned with also the precision syringe pump by using it in aspiration mode.
125   The flows were adjusted according to the desired dilution rate by using the neMESYS UserInterface
126   Software (Cetoni GmbH, Korbussen, Germany). The liquid handling was possible by using flexible
127   Teflon tubing and cannulas (Sterican; B. Braun Melsungen AG, Melsungen, Germany).

128   For the analysis of the glucose concentration, the effluent was passed into interchangeable
129   refrigerated sampling vessels. For rapid heat transfer, the sample vessels were cooled (Peltier
130   element) in an aluminum block, which caused the samples to freeze as soon as they contacted the
131   wall of the sampling vessels.

132   The µBC was equipped with miniaturised optical and electrochemical sensors that allowed real-time
133   online monitoring of the optical density (*OD*), dissolved oxygen (*DO)* and glucose concentration.

134

135   *2.2 Sensors*
136   *2.2.1 Optical density*

137   The *OD* of the biomass, which was measured at 600 nm ($OD_{\mu BC}$) during cultivation, was determined
138   online using an LED panel (EA LG40X21-A green-yellow, 51 × 21.2 × 4.8 mm, 8 V, Electronic
139   Assembly, Gilching, Germany) and a miniature spectrometer (USB 2000+, Ocean Optics, Ostfildern,
140   Germany) that was coupled to an optical fibre (200 µm diameter, M24L05, Thorlabs, Dachau,
141   Germany). The light intensity data was continuously measured every second and an average of ten
142   online monitoring points were recorded every 10 s with the SpectraSuite software (Ocean Optics,
143   Ostfildern, Germany). The $OD_{\mu BC}$ was calculated by:

144    $OD_{\mu BC} = ln\frac{I_0}{I}$ (1)

145   where I_0 and I are the light intensities measured through cell free cultivation medium and the cell
146   suspension, respectively.

147   A correlation between the $OD_{\mu BC}$ and optical density measured offline in the spectrophotometer
148   (OD_{photo}) needed to be determined for every cultivation. A linear correlation was then adjusted using

149 three pairs of *OD* measurement data (media, inoculum and final) and this enabled the conversion of
150 $OD_{\mu BC}$ to OD_{photo}.

151 A correlation between the OD_{photo} and biomass concentration, which was determined as the cell dry
152 weight (*CDW*) concentration (g/L) of *S. carnosus,* was derived from the measurements of samples
153 with known *CDW* concentrations and given by:

154 $$CDW_{concentration} = 0.0501 \cdot OD_{photo} \tag{2}$$

155 The *CDW* concentrations were determined by filling 10 mL of the cultivation broth in a test tube and it
156 was then centrifuged it at 3000 1/min for 10 min. The supernatant was removed and the pellet was
157 then resuspended in 10 mL of a 0.9 % (w/v) sodium chloride solution to remove the media residue. A
158 second centrifugation step was done, and the pellet was then dried at 105 °C until it achieved a
159 constant weight.

160 *2.2.2 Dissolved oxygen*

161 Online measurements of *DO* concentration were conducted using a microneedle oxygen sensor
162 (OXR50-CL4, Pyroscience, Aachen, Germany) with a response time < 2 s (liquid). This sensor was
163 introduced through the top of the *μBC* and connected to a four-channel phase-shift fluorimeter
164 (Firesting, Pyroscience, Aachen, Germany) and monitored by Pyro Oxygen Logger software
165 (PyroScience, Aachen, Germany).

166 *2.2.3 Glucose concentration*

167 The substrate-limiting carbon source of glucose, which is consumed by the cultivated cells, normally
168 requires sampling and bacterial removal to measure its concentration offline. However, in batch
169 experiments, it could be measured online using an electrochemical biosensor integrated in an
170 adjacent microfluidic chip as the sampling was not possible because of the small *μBC* volume.

171 Glucose depletion was measured by a glucose biosensor based on a *GOx* enzymatic electrochemical
172 biosensor as reported in Panjan et al. [25] and its integration and operation is described in Lladó
173 Maldonado et al. [22].

174 For the continuous experiments, it was possible to conduct an offline measurement of glucose of the
175 samples collected in the outlet. The measurement was performed with the glucose analyser
176 Kreienbaum YSI 2900/2950 (YSI Incorporated, Yellow Springs, Ohio, USA).

177 *2.3 Aerobic cultivation*

178 *2.3.1 Batch cultivation*

179 The cells were processed through all of the growth phases: lag, exponential, stationary and death
180 phase. The cell growth kinetics in the exponential phase in the batch cultivation can be described by:

181 $$\mu = \frac{1}{c_{CDW}} \cdot \frac{dc_{CDW}}{dt} \tag{3}$$

182   where μ (1/h) is the specific growth rate and c_{CDW} is the biomass concentration (g/L).

183

184   *2.3.2 Continuous cultivation*

185   Substrate-limited growth in a continuous cultivation is a process that allows the investigation of
186   stationary kinetic process parameters.

187   The biomass balance is:

188    $$\frac{dc_{CDW}}{dt} = D \cdot (c_{CDW,in} - c_{CDW}) + \mu \cdot c_{CDW} \qquad (4)$$

189   where the index "*in*" indicates the corresponding concentrations in the feed flow and the dilution rate
190   *D*, according to eq. (5), represents the quotient of the flow rate *F* and the reaction volume *V:*

191    $$D = \frac{F}{V} \qquad (5)$$

192   At steady state $\frac{dc_{CDW}}{dt} = 0$ and $c_{CDW,in} = 0$, the specific growth rate (μ) corresponds to the dilution rate
193   (*D)* according to:

194    $$\mu = D \qquad (6)$$

195   The mass balance for the limiting substrate concentration (c_S) can be expressed as:

196    $$\frac{dc_S}{dt} = D \cdot (c_{S,in} - c_S) - c_{CDW} \cdot \left(\frac{\mu}{Y_{X/S}} + m_s \right) \qquad (7)$$

197   where the yield coefficient, $Y_{X/S}$, corresponds to the substrate-related biomass yield, and m_S is the
198   coefficient of the endogenous maintenance metabolism of the cells.

199   Using the Monod model, μ can be expressed as in:

200    $$\mu = \frac{\mu_{max} \cdot c_S}{c_S + K_S} \qquad (8)$$

201   where μ_{max} is the maximum specific growth rate for a theoretical infinitely high substrate concentration
202   and the Monod constant, K_S, represents the substrate concentration corresponding to $1/2 \cdot \mu_{max}$. μ_{max}
203   and K_S were estimated with a non-linear fitting using the Monod growth function of OriginPro 2015
204   (OriginLab Corporation, Northampton, Massachusetts, USA).

205   The steady state biomass concentration c_{CDW} was isolated from eq. (7) and determined as function of
206   *D*:

207     $c_{CDW} = \dfrac{D \cdot (c_{S,in} - c_S)}{\dfrac{D}{Y_{X/S}} + m_s}$ (9)

208   The steady state substrate concentration, c_S, was obtained by applying eq. (6) in eq. (8) and then
209   determined as a function of D:

210     $c_S = \dfrac{D \cdot K_S}{\mu_{max} - D}$ (10)

211   When $D \geq D_{washout}$, the biomass would be washed out of the reactor system. The substrate
212   concentration would increase as $D \rightarrow D_{washout}$ and the glucose concentration would reach its input
213   value $c_{S,in}$ at $D_{washout}$ as described in:

214     $D_{washout} = \dfrac{\mu_{max} \cdot c_{S,in}}{c_{S,in} + K_S}$ (11)

215   The maximal specific growth rate μ_{max} would theoretically be achieved if the substrate concentration
216   were infinitely large. Therefore, $D_{washout} < \mu_{max}$.

217   The specific substrate uptake rate q_S can be expressed as:

218     $q_S = \dfrac{D \cdot (c_{S,in} - c_S)}{c_{CDW}} = \dfrac{D}{Y_{X/S}} + m_s$ (12)

219   By using eq. (12), $Y_{X/S}$ and m_S can be determined from the slope and the ordinate intercept,
220   respectively.

221   The biomass-related productivity (Pr) can be obtained by combining eq. (9) and (10) and neglecting
222   m_S:

223     $Pr = D \cdot c_{CDW} = D \cdot Y_{X/S} \cdot \left(c_{S,in} - \dfrac{D \cdot K_S}{\mu_{max} - D} \right)$ (13)

224   The value of D at which the productivity of the cell mass is maximised, which is defined as $D_{Pr,\,max}$, is
225   obtained when $dPr\,/\,dD = 0$ and is calculated as follows:

226     $D_{Pr,\,max} = \mu_{max} \cdot \left(1 - \sqrt{\dfrac{K_S}{K_S + c_{S,in}}} \right)$ (14)

227   *2.3.3 Strain, inoculum and cultivation medium*

228   The *Staphylococcus carnosus* TM300 GFP strain was used and contained the plasmid pCX-pp-
229   sfGFP, which carries information to produce the green fluorescence protein (*GFP*) [26–28].The
230   cultivations of *S. carnosus* were performed in a complex media [24] with 1 g/L glucose and 10 µg/mL
231   chloramphenicol as an antibiotic, at 30 ºC, with a pH value of 6.4 and with an aeration corresponding
232   to a superficial gas velocity of $2.25 \cdot 10^{-3}$ m/s. The inoculum of *S. carnosus* was prepared from cryo-

233   cultures stored in glycerol at −80 °C. The cells were reactivated by overnight growth in a shaken flask

234   with 25 mL of the complex media but with 10 g/L glucose at 30 ºC and 180 1/min (25 mm eccentricity),

235   and the cultivations were then started in the μBC and diluted to an OD of 0.2 when measured at

236   600 nm (OD_{photo}) (Spectrophotometer Libra S 11, Biochrom, Cambridge, UK).

237

238   **3 Results and Discussion**

239   The application of the present study was to validate the functionality of the novel μBC as a tool for

240   screening reaction kinetics in the batch and chemostat conditions. The batch cultivation of *S. carnosus*

241   was performed in the μBC with online monitoring of OD, DO and glucose concentration over the entire

242   cultivation time.

243   In **Fig. 2**, the batch cultivation *of S. carnosus* over time for one of the cultivation replicates is

244   presented. After an initial lag phase, there was a phase of exponential growth with a maximum growth

245   rate of μ= 0.39 1/h and reached a final biomass concentration of 0.27 g/L after 8 h of cultivation, where

246   the glucose was fully depleted from the cultivation medium. The DO decreased slightly during the

247   exponential phase, and increased again during the stationary phase. The cultivation medium was

248   almost saturated during the whole cultivation. The maximal growth rate, μ_{max}, values were determined

249   via batch cultivation of *S. carnosus* and can be found in the literature. μ_{max} was reported in Davies et

250   al. [24] using an 150 µL horizontal *MBR* with μ_{max}= 0.60 1/h and in shaken flask μ_{max}= 0.65 1/h using

251   the same medium as this study. In a miniaturised bubble column-bioreactor with a volume of 200 -

252   400 mL Dilsen [29] determined a μ_{max}= 0.75 1/h for this strain.

253   The DO was additionally measured at certain points of the cultivation to prove that an adequate

254   oxygen supply was always guaranteed (**Fig. 3**). At dilution rates below 0.6 1/h and where the CDW

255   concentration was higher, there was a higher oxygen consumption, which led to a DO of 60 - 70 %,

256   whereas when the cultivation was working at higher dilution rates, the DO increased to 90 % and this

257   was due to the reduction of the biomass concentration. Overall, the DO levels were more than

258   sufficient to guarantee the optimal growth of *S. carnosus* without oxygen limitations.

259   The samples at each dilution rate were collected into a sampling vessel after at least three residence

260   times, at the respective dilution rate. The OD_{photo} was converted to biomass concentration (CDW

261   concentration) with the correlation described in eq. (2).

262   Fig. 3 shows that in the dilution rate range of D = 0.15 - 0.55 1/h, the CDW concentration stayed

263   approximately constant at 0.3 g/L. At D ≥ 0.6 1/h, the stationary CDW concentrations reached lower

264   values. The reduction of the biomass concentration was reflected in lower glucose consumption. The

265   biomass-related productivity was determined with eq. (13).

266   From the stationary glucose concentration data obtained at the different dilution rates, the Monod

267   growth kinetic parameters, μ_{max} and K_S, were estimated (**Fig. 4**) with the Levenberg-Marquardt non-

268   linear least squares algorithm for iteration and this resulted in μ_{max}= 0.824 ± 0.007 1/h and

269     $K_S = 34 \cdot 10^{-3} \pm 2 \cdot 10^{-3}$ g$_S$/L (R^2 = 0.991). K_S describes the affinity of the organism to the substrate with

270   high affinities for low values. The estimated $K_S = 34 \cdot 10^{-3}$ g/L indicates a high affinity of *S. carnosus*

towards glucose. In **Tab. 1**, the K_S and μ_{max} values that were determined via the traditional linearization methods of Lineweaver-Burk, Eadie-Hofstee and Hanes-Woolf are shown and demonstrate a good accordance between them and with the before-mentioned non-linear fitting method.

Tab. 2 shows some values for the Monod constant K_S for growth on different substrates for different strains. Typical examples of the state of information on the kinetic properties exhibited by a particular microorganism are the data available for *Escherichia coli* and *Saccharomyces cerevisiae* growing with glucose. The K_S values reported vary over more than 2 and 3 orders of magnitude, and it should be stressed that the case of *E. coli* and *S. cerevisiae* does not stand alone. For the case of *S. carnosus* ($K_S = 34 \cdot 10^{-3}$ g/L) with glucose as growth limiting carbon source the estimated K_S value appears to be in a trusted area, with which further kinetic modeling is on a fair fundament.

The data of the biomass and substrate concentration were used to calculate the yield coefficient, $Y_{X/S}$, and the maintenance, m_S, with eq. (12) by plotting the specific consumption rate, q_S, against D (**Fig. 5**). Using eq. (12), $Y_{X/S}$ and m_S can be determined from the slope and the ordinate intercept as 0.315 g_{CDW}/g_S and 0.0035 $g_S/(g_{CDW}$ h), respectively. In **Fig. 6**, the calculated data (solid lines) are based on the reaction kinetic model using the steady state cell dry weight concentration (c_{CDW}), glucose concentration (c_S) and biomass-related productivity (Pr) according to eq. (9), (10) and (13), respectively. The measured experimental data for the continuous cultivation of *S. carnosus* as a function of the dilution rate D are depicted. The parameters used in the reaction kinetic model were: $c_{S,in} = 1$ g_S/L, $\mu_{max} = 0.824$ 1/h, $K_S = 34 \cdot 10^{-3}$ g/L, $Y_{X/S} = 0.315$ g_{CDW}/g_S, and $m_S = 0.0035$ $g_S/(g_{CDW} \cdot h)$.
The dilution rate with highest biomass-related productivity, $D_{Pr,max}$, was determined with eq. (14) and with $D_{Pr,max} = 0.675$ 1/h. The corresponding maximum cell productivity resulted in 0.18 $g_{CDW}/(L \cdot h)$. The washout value, $D_{washout}$, was calculated using eq. (11) as $D_{washout} = 0.797$ 1/h. The experimental points fitted very well to the estimated theoretical trends of biomass, glucose and productivity as well as $D_{Pr,max}$ and $D_{washout}$ calculated from the Monod based reaction kinetic model. With this experiment, the *µBC* was proven successful for estimating growth kinetics rapidly and cost-effectively with continuous cultivations.

4 Conclusions

In the present work, the applicability of a novel, sensor-integrated multiphase *MBR* was investigated. The developed *µBC* had a reaction volume of 550 µL and was aerated and mixed by the continuous flow of microbubbles generated in the nozzle. The *µBC* was prepared for the online monitoring of process parameters (*OD, DO* and glucose) through integrated optical chemical and electrochemical sensors that provided a comprehensive knowledge of the bioprocess. In this work, the application of a functional, cost-effective *µBC* with a rapid setup, as a platform for aerobic cultivation of biological systems in batch and chemostat mode for the determination of kinetic parameters is presented.

The applicability of the *µBC* for submerged whole-cell cultivation in chemostat mode could be demonstrated by cultivating *S. carnosus* and by reaching steady state concentrations of biomass and substrate at different dilution rates. For the first time, the growth kinetic parameters of *S. carnosus*

309   were estimated from stationary data pairs of biomass and substrate concentration obtained from
310   continuous cultivation and with μ_{max} = 0.824 1/h, K_S = 34 · 10^{-3} g/L, $Y_{X/S}$ = 0.315 g_{CDW}/g_S, and
311   m_S = 0.0035 $g_S/(g_{CDW}\cdot h)$.

312   The current μBC fits with the challenges of sensing technology, control strategy and standardization
313   for the successful implementation of microfluidic devices in bioprocessing, and therefore the μBC can
314   be more efficiently applied in bioprocessing. Further studies should focus on the integration of more
315   online sensors for other substrates and products in the μBC. The sensing technology could further be
316   extended if the μBC were integrated within a robotic platform with at- and offline analytical equipment
317   to enlarge the amount of available process information. The system should be designed with a higher
318   degree of parallelisation to fill the high throughput gap.

319

327

328   **Abbreviations**

329   *GOx*   glucose oxidase

330   *MBR*   microbioreactor

331   *PDMS*   polydimethylsiloxane

332   *PMMA*   polymethyl methacrylate

333   *µBC*   microbubble column-bioreactor

334

335   **Nomenclature**

336   *CDW*   cell dry weight (g)

337   c_S substrate concentration (g/L)

338   c_{CDW} biomass concentration (g/L)

339   *D*   dilution rate (1/h)

340   *DO*   dissolved oxygen (%)

341   *F*   flow rate (L/h)

342	$k_L a$	volumetric liquid-phase mass transfer coefficient (1/h)
343	K_S	Monod constant (g/L)
344	m_S	maintenance coefficient ($g_S/(g_{CDW} \cdot h)$)
345	OD	optical density (-)
346	Pr	biomass-related productivity ($g_{CDW}/(L \cdot h)$)
347	q_S	specific substrate uptake rate ($g_S/(g_{CDW} \cdot h)$)
348	V	reaction volume (L)
349	$Y_{X/S}$	substrate-related biomass yield coefficient (g_{CDW}/g_S)
350	μ	specific growth rate (1/h)

References

351

352   1.   Kirk T V, Szita N (2013) Oxygen transfer characteristics of miniaturized bioreactor systems.
353   Biotechnol Bioeng 110:1005–1019 . doi: 10.1002/bit.24824

354   2.   Krull R, Lladó Maldonado S, Lorenz T, et al (2016) Microbioreactors. In: Dietzel A (ed)
355   Microsystems for Pharmatechnology. Manipulation of fluids, particles, droplets, and cells.
356   Springer International Publishing, Cham Heidelberg New York Dordrecht London, pp 99–152

357   3.   Marques MPC, Szita N (2017) Bioprocess microfluidics : applying microfluidic devices for
358   bioprocessing. Curr Opin Chem Eng 18:61–68 . doi: 10.1016/j.coche.2017.09.004

359   4.   Gruber P, Marques MPC, Szita N, Mayr T (2017) Integration and application of optical chemical
360   sensors in microbioreactors. Lab Chip 17:2693–2712 . doi: 10.1039/C7LC00538E

361   5.   Lasave LC, Borisov SM, Ehgartner J, Mayr T (2015) Quick and simple integration of optical
362   oxygen sensors into glass-based microfluidic devices. RSC Adv 5:70808–70816 . doi:
363   10.1039/C5RA15591F

364   6.   Ehgartner J, Sulzer P, Burger T, et al (2016) Online analysis of oxygen inside silicon-glass
365   microreactors with integrated optical sensors. Sensors Actuators B Chem 228:748–757 . doi:
366   10.1016/j.snb.2016.01.050

367   7.   Pfeiffer SA, Nagl S (2015) Microfluidic platforms employing integrated fluorescent or
368   luminescent chemical sensors: a review of methods, scope and applications. Methods Appl
369   Fluoresc 3:34003 . doi: 10.1088/2050-6120/3/3/034003

370   8.   Panjan P, Virtanen V, Sesay AM (2018) Towards microbioprocess control: An inexpensive 3D
371   printed microbioreactor with integrated online real-Time glucose monitoring. Analyst 143:3926–
372   3933 . doi: 10.1039/c8an00308d

373   9.   Bolic A, Larsson H, Hugelier S, et al (2016) A flexible well-mixed milliliter-scale reactor with
374   high oxygen transfer rate for microbial cultivations. Chem Eng J 303:655–666 . doi:
375   10.1016/j.cej.2016.05.117

376   10.   Peterat G, Schmolke H, Lorenz T, et al (2014) Characterization of oxygen transfer in vertical
377   microbubble columns for aerobic biotechnological processes. Biotechnol Bioeng 111:1809–
378   1819 . doi: 10.1002/bit.25243

379   11.   Zhang Z, Szita N, Boccazzi P, et al (2005) A well-mixed, polymer-based microbioreactor with
380   integrated optical measurements. Biotechnol Bioeng 93:286–296 . doi: 10.1002/bit.20678

381   12.   Schäpper D, Stocks SM, Szita N, et al (2010) Development of a single-use microbioreactor for
382   cultivation of microorganisms. Chem Eng J 160:891–898 . doi: 10.1016/j.cej.2010.02.038

383   13.   Kostov Y, Harms P, Randers-Eichhorn L, Rao G (2001) Low-cost microbioreactor for high-
384   throughput bioprocessing. Biotechnol Bioeng 72:346–352 . doi: 10.1002/1097-
385   0290(20010205)72:3<346::AID-BIT12>3.0.CO;2-X

386 14. Zanzotto A, Szita N, Boccazzi P, et al (2004) Membrane-aerated microbioreactor for high-
387   throughput bioprocessing. Biotechnol Bioeng 87:243–254 . doi: 10.1002/bit.20140

388 15. Kirk TV, Marques MPC, Radhakrishnan ANP, Szita N (2016) Quantification of the oxygen
389   uptake rate in a dissolved oxygen controlled oscillating jet-driven microbioreactor. J Chem
390   Technol Biotechnol 91:823–831 . doi: 10.1002/jctb.4833

391 16. Marbà-Ardébol AM, Emmerich J, Muthig M, et al (2018) Real-time monitoring of the budding
392   index in *Saccharomyces cerevisiae* batch cultivations with in situ microscopy. Microb. Cell
393   Fact. 17:73

394 17. Klein T, Schneider K, Heinzle E (2013) A system of miniaturized stirred bioreactors for parallel
395   continuous cultivation of yeast with online measurement of dissolved oxygen and off-gas.
396   Biotechnol Bioeng 110:535–42 . doi: 10.1002/bit.24633

397 18. Krull R, Peterat G (2016) Analysis of reaction kinetics during chemostat cultivation of
398   *Saccharomyces cerevisiae* using a multiphase microreactor. Biochem Eng J 105:220–229 .
399   doi: 10.1016/j.bej.2015.08.013

400 19. Edlich A, Magdanz V, Rasch D, et al (2010) Microfluidic reactor for continuous cultivation of
401   *Saccharomyces cerevisiae*. Biotechnol Prog 26:1259–1270 . doi: 10.1002/btpr.449

402 20. Zhang Z, Boccazzi P, Choi H-G, et al (2006) Microchemostat-microbial continuous culture in a
403   polymer-based, instrumented microbioreactor. Lab Chip 6:906–913 . doi: 10.1039/b518396k

404 21. Lladó Maldonado S, Rasch D, Kasjanow A, et al (2018) Multiphase microreactors with
405   intensification of oxygen mass transfer rate and mixing performance for bioprocess
406   development. Biochem Eng J 139:57–67 . doi: 10.1016/j.bej.2018.07.023

407 22. Lladó Maldonado S, Panjan P, Sun S, et al (2019) A fully online sensor-equipped, disposable
408   multiphase microbioreactor as a screening platform for biotechnological applications.
409   Biotechnol Bioeng 116:65–75 . doi: https://doi.org/10.1002/bit.26831

410 23. Löfblom J, Rosenstein R, Nguyen MT, et al (2017) *Staphylococcus carnosus*: from starter
411   culture to protein engineering platform. Appl Microbiol Biotechnol 101:8293–8307 . doi:
412   10.1007/s00253-017-8528-6

413 24. Davies MJ, Nesbeth DN, Szita N (2013) Development of a microbioreactor "cassette" for the
414   cultivation of microorganisms in batch and chemostat mode. Chim Oggi - Chem Today 31:46–
415   49

416 25. Panjan P, Virtanen V, Sesay AM (2017) Determination of stability characteristics for
417   electrochemical biosensors via thermally accelerated ageing. Talanta 170:331–336

418 26. Mauthe M, Yu W, Krut O, et al (2012) WIPI-1 positive autophagosome-like vesicles entrap
419   pathogenic Staphylococcus aureus for lysosomal degradation. Int J Cell Biol 2012:179207 .
420   doi: 10.1155/2012/179207

421   27.   Rosenstein R, Nerz C, Biswas L, et al (2009) Genome analysis of the meat starter culture
422   bacterium *Staphylococcus carnosus* TM300. Appl Environ Microbiol 75:811–822 . doi:
423   10.1128/AEM.01982-08

424   28.   Yu W, Götz F (2012) Cell wall antibiotics provoke accumulation of anchored mCherry in the
425   cross wall of Staphylococcus aureus. PLoS One 7:e30076 . doi: 10.1371/journal.pone.0030076

426   29.   Dilsen S, Paul W, Herforth D, et al (2001) Evaluation of parallel operated small-scale bubble
427   columns for microbial process development using *Staphylococcus carnosus*. J Biotechnol
428   88:77–84 . doi: 10.1016/S0168-1656(01)00265-6

429   30.   Atkinson B, Mavituna F (1991) Biochemical Engineering and Biotechnology Handbook, 2nd ed.
430   Stockton Press, New York

431   31.   Kovárová-Kovar K, Egli T (1998) Growth kinetics of suspended microbial cells: from single-
432   substrate-controlled growth to mixed-substrate kinetics. Microbiol Mol Biol Rev 62:646–666

433   32.   Krull R, Hempel DC (1994) Biodegradation of naphthalenesulphonic acid-containing sewages
434   in a two-stage treatment plant. Bioprocess Eng 10:229–234 . doi: 10.1007/BF00369534

435   33.   Rieger M, Käppeli O, Fiechter A (1983) The role of limited respiration in the incomplete
436   oxidation of glucose by *Saccharomyces cerevisiae*. J Gen Microbiol 129:653–661 . doi:
437   10.1099/00221287-129-3-653

438   34.   von Meyenburg HK (1969) Energetics of the budding cycle of *Saccharomyces cerevisiae*
439   during glucose limited aerobic growth. Arch Mikrobiol 66:289–303 . doi: 10.1007/BF00414585

440   35.   von Meyenburg K (1969) Katabolit-Repression und der Sprossungszyklus von *Saccharomyces*
441   *cerevisiae*. PhD thesis, ETH Zürich

442

443

444 **Tables and Figures**

445 **Table 1.** The kinetic parameters maximum specific growth rate, μ_{max}, and the Monod constant, K_S,
446 determined by different linearization methods and non-linear fitting.

Method / Parameter	μ_{max} (1/h)	K_S ($10^{-3} \cdot$ g/L)	R^2
Lineweaver-Burk	0.823	33	0.992
Eadie-Hofstee	0.823	34	0.989
Hanes-Woolf	0.827	36	0.999
Monod non linear fitting	0.824	34	0.991

447
448

449 **Table 2.** Comparison of Monod constant K_S values for growth on different substrates.

Microorganism	Substrate	K_S ($10^{-3} \cdot$ g/L)	Reference
S. carnosus	Glucose	34.0	This work
Candida	Glycerol	4.5	Atkinson and Mavituna [30]
	Oxygen	0.45	
	Ammonia	0.1	
Escherichia coli	Glucose	2.0 – 4.0	Kovárová-Kovar and Egli [31]
		20 – 100	
	Lactose	20.0	Atkinson and Mavituna [30]
	Mannitol	2.0	
	Phosphate	1.6	
	Trytophan	0.001	
Hansenula polymorpha	Methanol	120.0	
	Ribose	3.0	
Klebsiella sp.	Carbon dioxide	0.4	
	Magnesium	0.6	
	Potassium	0.4	
	Sulphate	2.7	
Pseudomonas sp.	Methane	0.7	
	Methanol	0.4	
	Naphthalene sulfonic acid	5.3	Krull and Hempel [32]
Saccharomyces cerevisiae	Glucose	25.0	Atkinson and Mavituna [30]
		182	Krull and Peterat [18]
		13.0 – 234.0	Rieger et al. [33]
		22	Von Meyenburg [34, 35]

450

451

452

Figure 1. Picture of the *µBC* and its setup. The inlets and outlets of the liquid and gas phases are illustrated with arrows that show the direction of the flow. The labels also indicate the integrated sensors dissolved oxygen and optical density with their associated glass fibers, and the microfluidic flow chip with the integrated glucose biosensor.

457
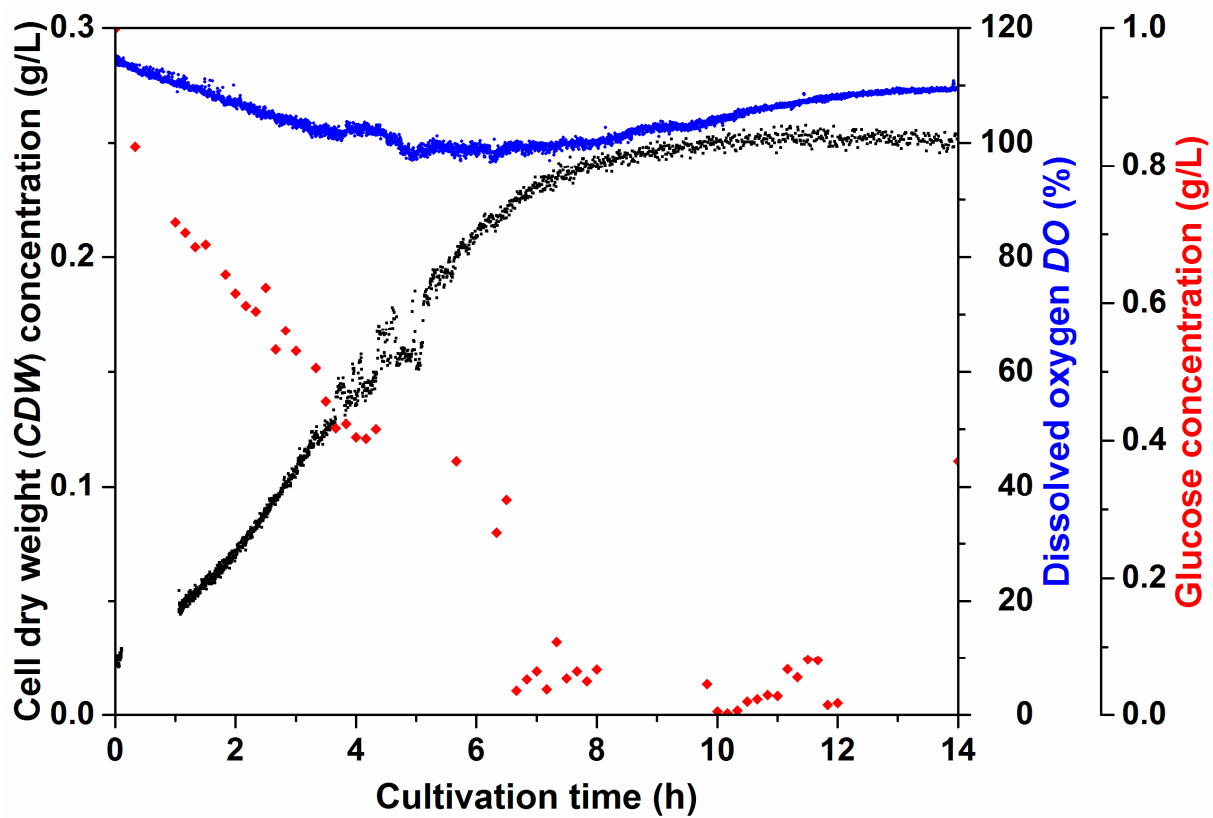
Figure 2. Batch cultivation of *Staphylococcus carnosus* in the cuvette-based microbubble column-bioreactor (*µBC*) with measurement of the cell dry weight (*CDW*) concentration (■), dissolved oxygen (*DO*) (●), and glucose concentration (♦) over time.
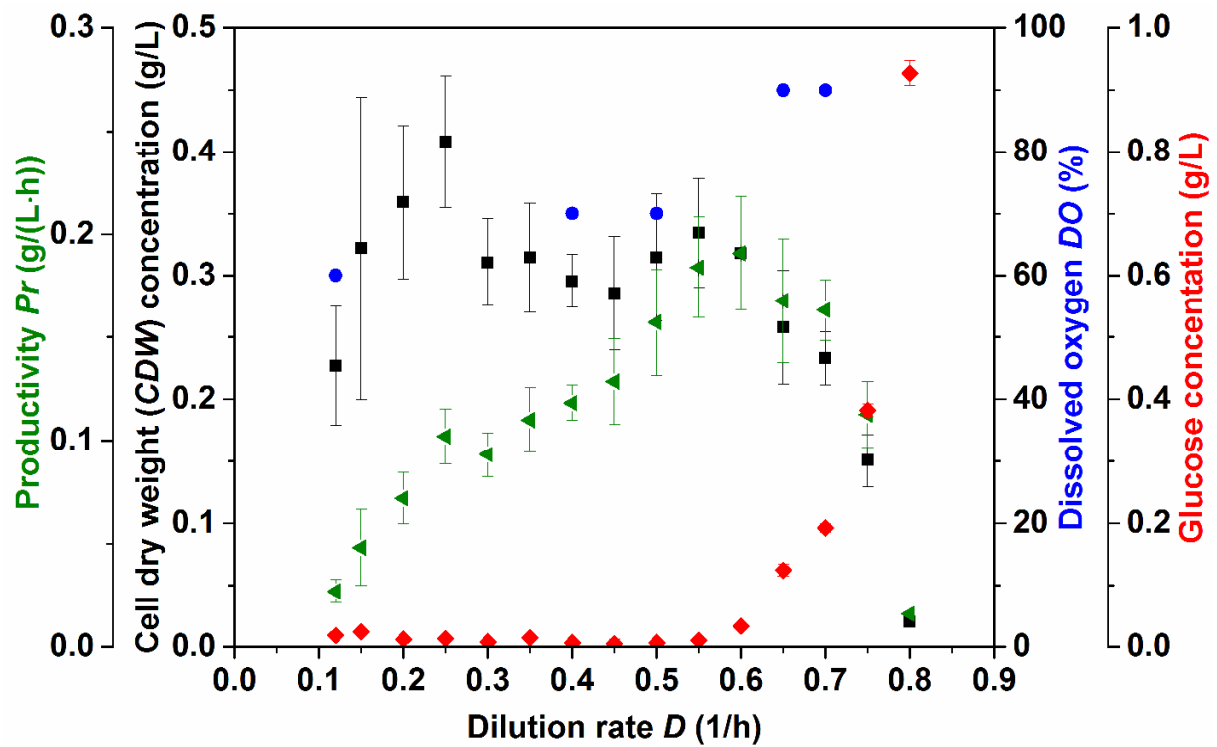
464
465 **Figure 3.** Continuous cultivation of *Staphylococcus carnosus* at different dilution rates from *D*= 0.12 to
466 0.80 1/h with a glucose-feed concentration of 1 g/L. Determined stationary concentrations of the cell
467 dry weight (*CDW*) concentration (■), dissolved oxygen (*DO*) (●), glucose concentration (♦) and
468 biomass-related productivity (◄) were calculated by eq. (13).
469
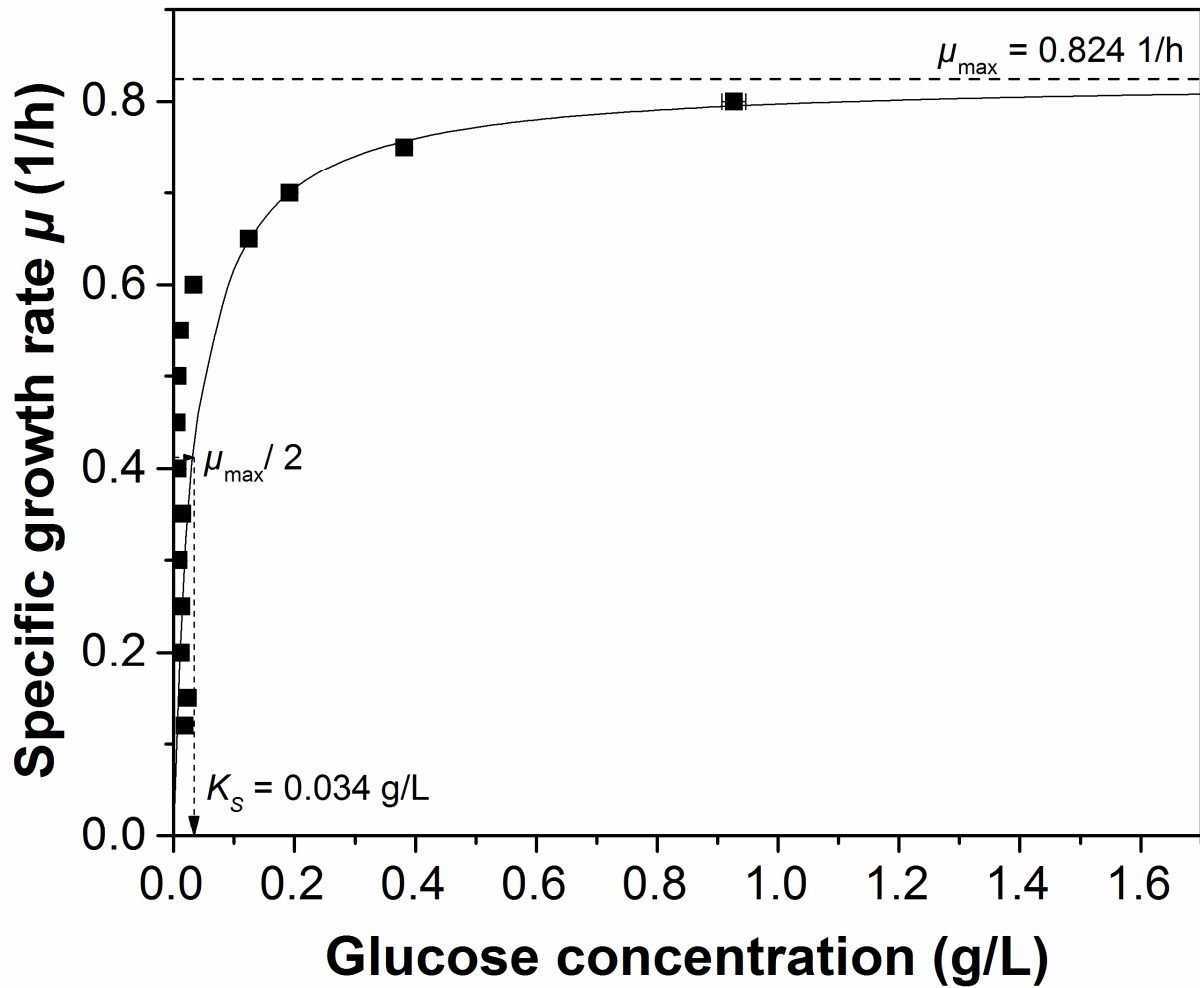
Figure 4. Monod growth kinetic parameter estimation by fitting the experimental stationary glucose concentrations measured during the continuous cultivation of *Staphylococcus carnosus* (cultivation temperature 30 °C and *pH* value= 6.4) with a glucose-feed concentration of 1 g/L at different dilution rates, which resulted in a maximum specific growth rate μ_{max}= 0.824 ± 0.007 1/h and a Monod constant K_S = (34± 2) $\cdot 10^{-3}$ g$_S$/L (R^2= 0.991).
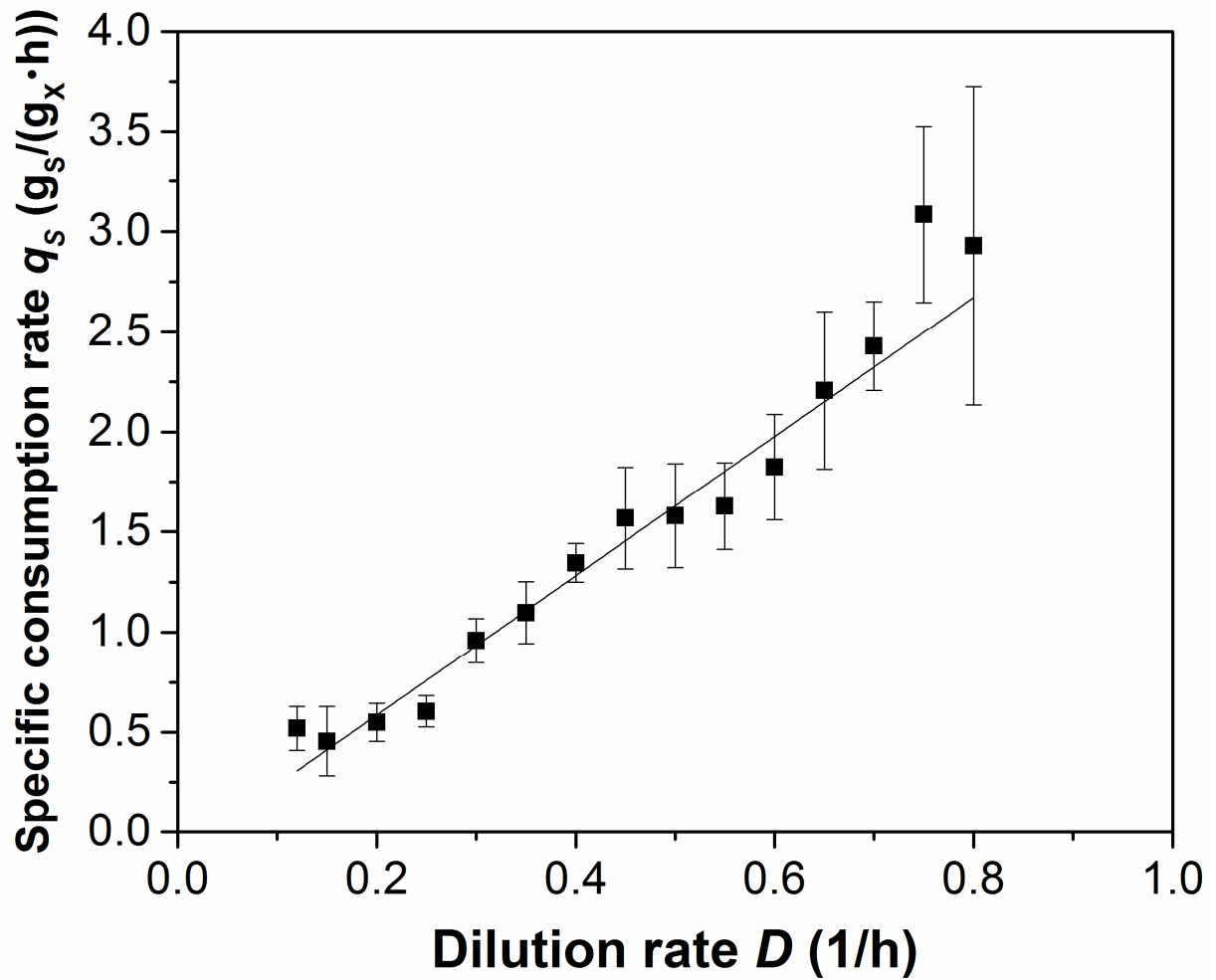
Figure 5. The stationary specific substrate consumption rate q_S (calculated by eq. (12)) during the continuous cultivation of *Staphylococcus carnosus* at different dilution rates. By performing a linear regression analysis of the plotted data, the substrate-related biomass yield coefficient $Y_{X/S}$= 0.315 g_{CDW}/g_S (the inverse of the slope) and the maintenance coefficient m_S= 0.0035 $g_S/(g_{CDW} \cdot h)$ (from the intercept) were calculated (R^2= 0.983).

484
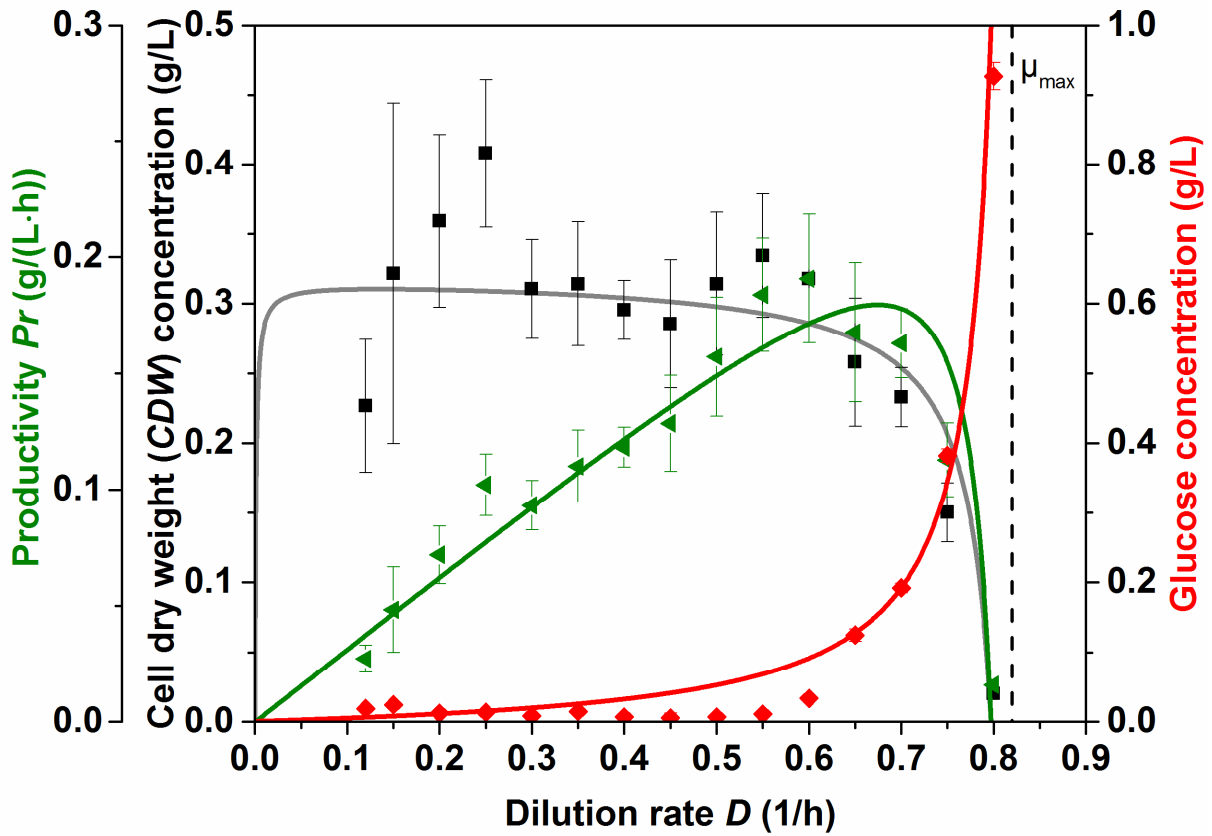
Figure 6. Comparison of the Monod-based reaction kinetic model using the steady state cell dry weight concentration (c_{CDW}), glucose concentration (c_S) and biomass-related productivity (Pr) according to eq. (9), (10) and (13), respectively, with the experimental data (c_S, ♦; c_{CDW}, ■; and Pr, ◄) for the continuous cultivation of *Staphylococcus carnosus,* as a function of the dilution rate D. The parameters used in the reaction kinetic model were $c_{S,in}$ = 1 g_S/L, μ_{max} = 0.824 1/h, K_S = 34·10^{-3} g_S/L, $Y_{X/S}$ = 0.315 g_{CDW}/g_S, and m_S = 0.0035 g_S/(g_{CDW}·h). The dashed vertical line indicates μ_{max} = 0.824 1/h.